Supplementary Material

Janus hydrogel-based fuel stimulant powered amplification for multiple detections of miRNA biomarkers in gastric cancer.

Jaewoo Lim[a,c,+], *Jin-Seong Hwang*[b,d,+], *Seung Beom Seo*[a,e], *Byunghoon Kang*[a], *Soojin Jang*[a,c], *Seong Uk Son*[a,c], *Jisun Ki*[a], *Jang-Seong Kim*[b,d], *Taejoon Kang*[a], *Juyeon Jung*[a,c], *Tae-Su Han*[b,d,*], *Eun-Kyung Lim*[a,c,*]

[a]Bionanotechnology Research Center, Korea Research Institute of Bioscience and Biotechnology (KRIBB), 125 Gwahak-ro, Yuseong-gu, Daejeon, 34141, Republic of Korea

[b]Biotherapeutics Translational Research Center, Korea Research Institute of Bioscience and Biotechnology (KRIBB), 125 Gwahak-ro, Yuseong-gu, Daejeon 34141, Republic of Korea

[c]Department of Nanobiotechnology, KRIBB School of Biotechnology, University of Science and Technology, 125 Gwahak-ro, Yuseong-gu, Daejeon, 34113, Republic of Korea

[d]Department of Functional Genomics, KRIBB School of Bioscience, University of Science and Technology, 125 Gwahak-ro, Yuseong-gu, Daejeon, 34113, Republic of Korea

[e]Department of Cogno-Mechatronics Engineering, Pusan National University, 2 Busandaehak-ro 63beon-gil, Geumjeong-gu, Busan 46241, Republic of Korea.

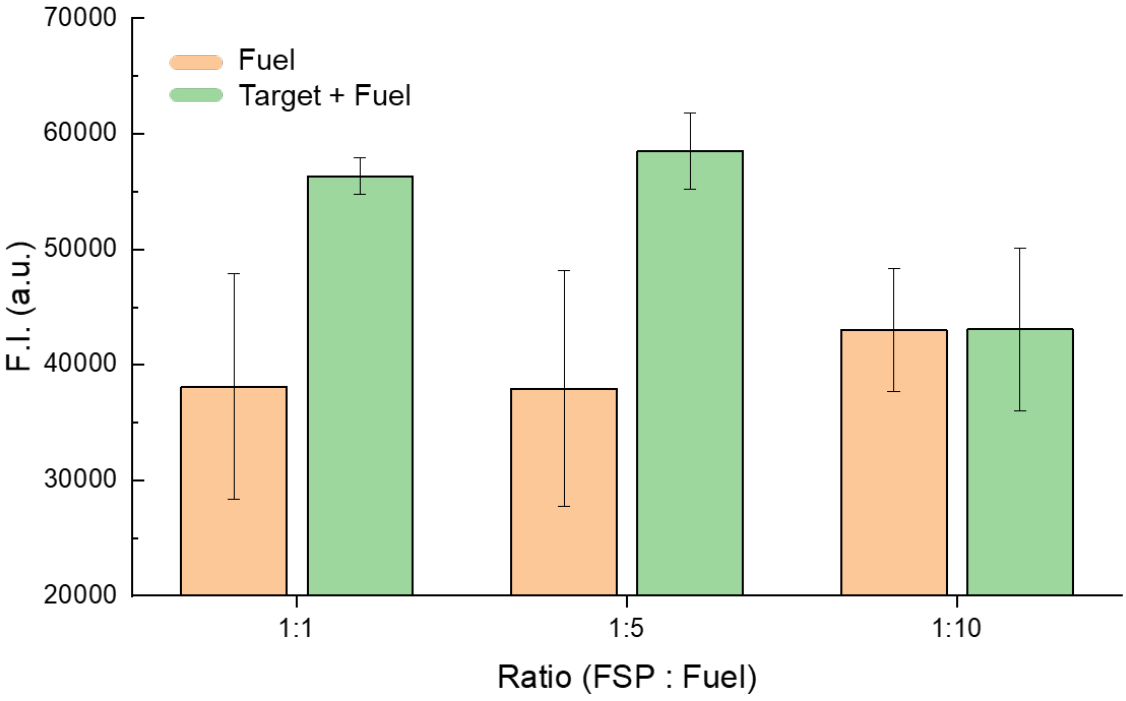

Figure S1. Optimization of the fuel concentration. This graph presents the fluorescence intensities of 100 nM fuel stimulant-powered (FSP) probes in the presence of 1 nM synthetic target and various concentration/ratios of the fuel [100 nM (1:1), 500 nM (1:5), and 1 uM (1:10)]. These intensities were measured following 2 h incubation at room temperature.

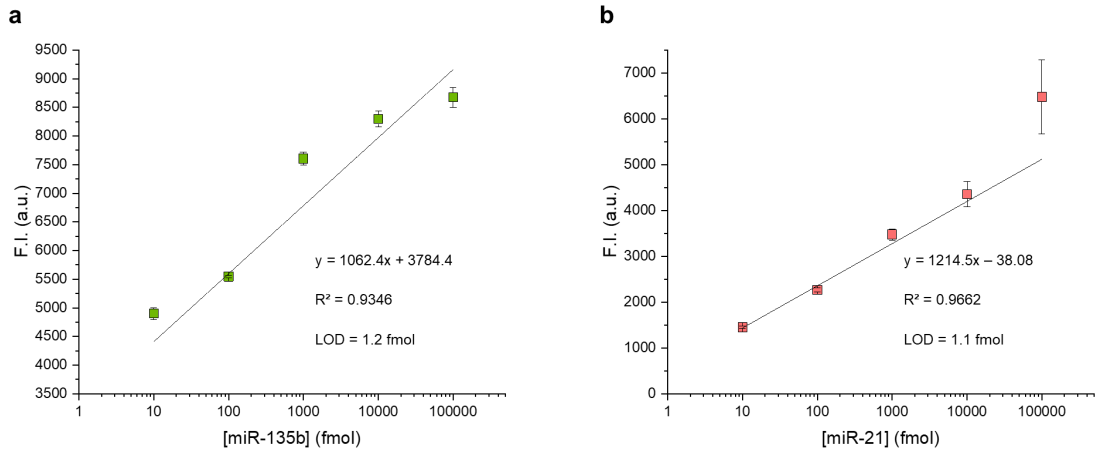

Figure S2. Calibration curves of a) FSP-135b and b) FSP-21 in solution

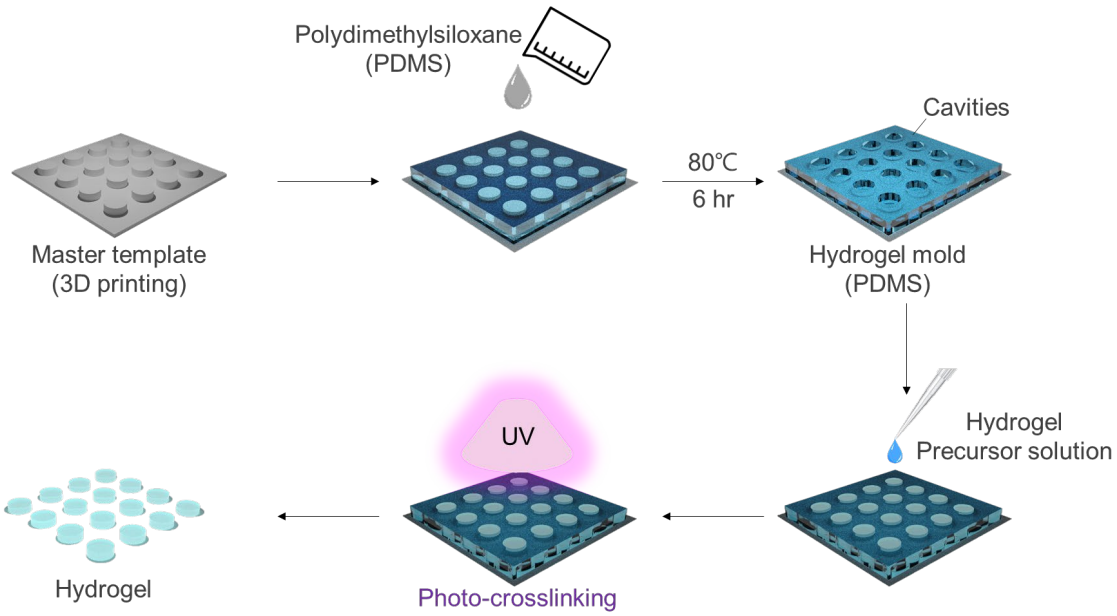

Figure S3. Schematic illustration of stepwise fabrication of the hydrogel molds and the subsequent synthesis of cylindrical hydrogels.

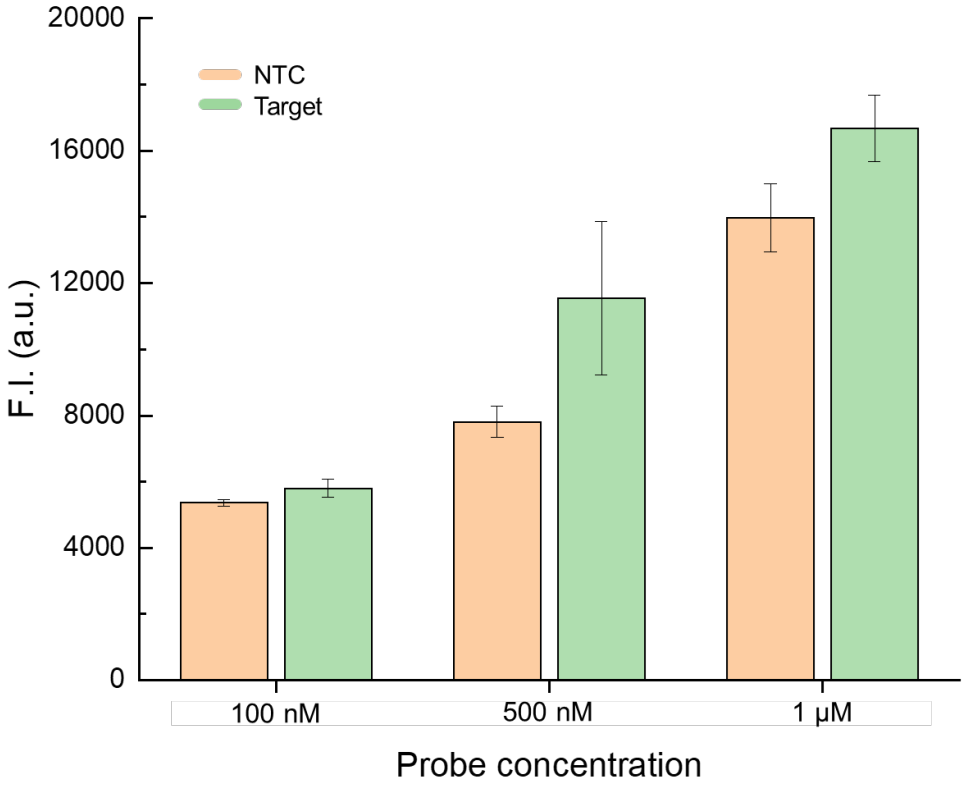

Figure S4. Fluorescence intensities (F.I.) of hydrogels containing various concentrations of fuel stimulant-powered probes (100 nM, 500 nM, and 1 μM) and 1 nM of the synthetic target and 1:1 ratio of the fuel. NTC indicates sample containing no target sequence. These intensities were measured following 2 hrs incubation at room temperature.

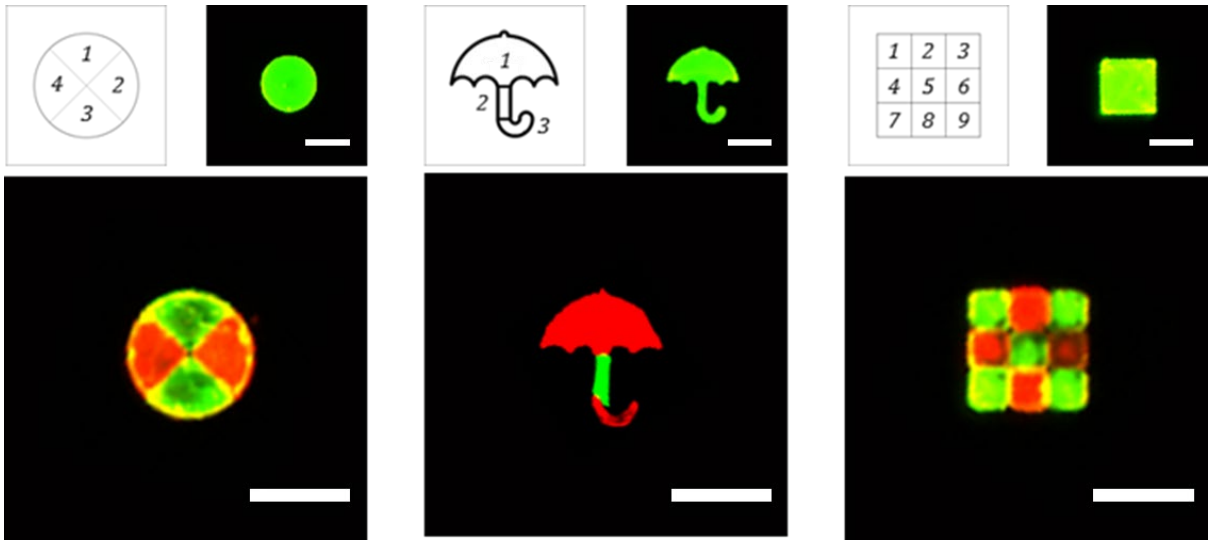

Figure S5. Fluorescence images of different hydrogel patterns. These poly(ethylene glycol) hydrogels of various shapes were synthesized by photolithography (scale bar: 5 mm).

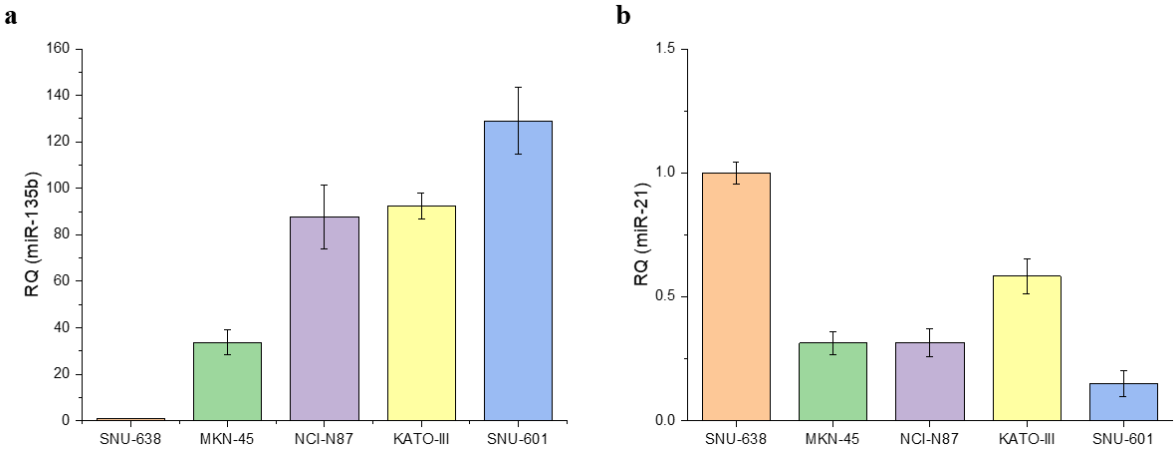

Figure S6. Real-time PCR analyses of (a) miR-135b and (b) miR-21 expression levels in five gastric cancer cell lines. Expression levels of the miRNAs were normalized to that of RNU6B (n = 3). RQ, Relative quantification.

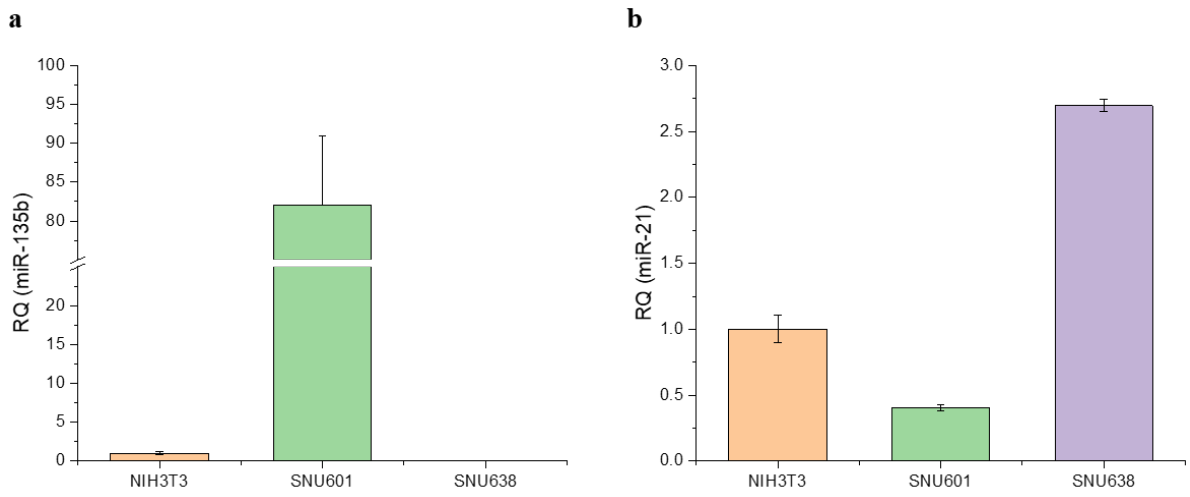

Figure S7. Real-time PCR analyses of (a) miR-135b and (b) miR-21 expression levels in mammalian cells. Expression levels of the miRNAs were normalized to that of RNU6B ($n = 3$). RQ, Relative quantification; NIH3T3, normal mouse fibroblasts; SNU601 and SNNU638, gastric cancer cells.

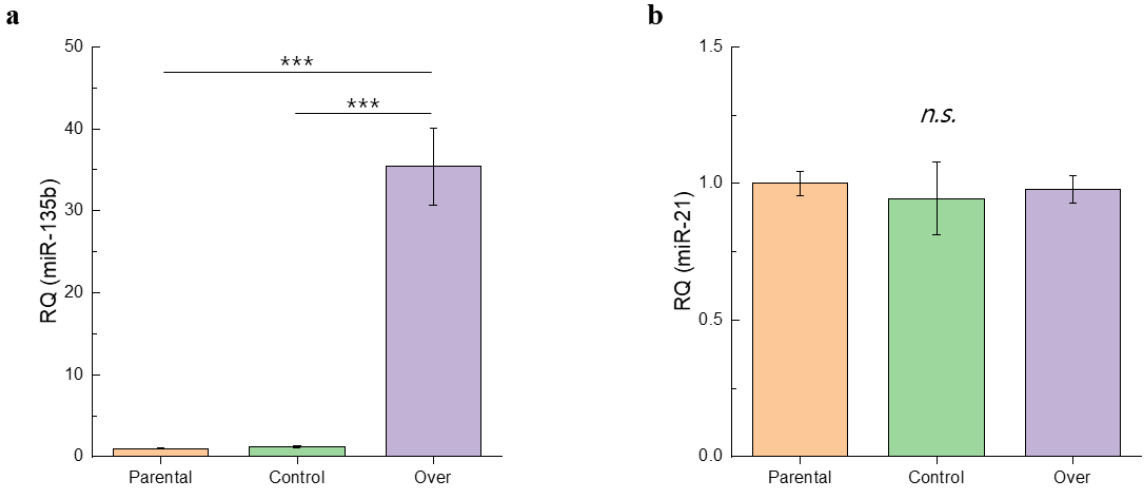

Figure S8. Real-time PCR analyses of (a) miR-135b and (b) miR-21 expression levels in SNU638 (parental), SNU638_control (control), and SNU638_over (miR-135b overexpression, Over) cells. Expression levels of the miRNAs were normalized to that of RNU6B (n = 3). RQ, Relative quantification.

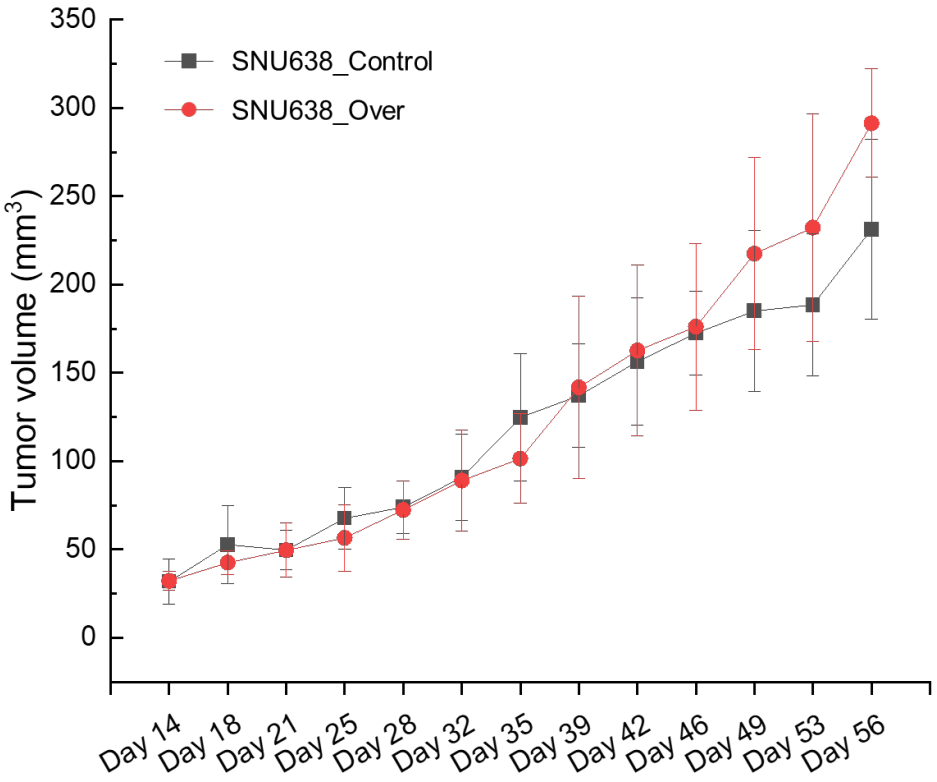

Figure S9. Tumor volumes of xenograft mouse models measured biweekly and estimated using the formula: volume = length × width^2/2. Data is expressed as mean ± standard deviation (SD) of five mice.

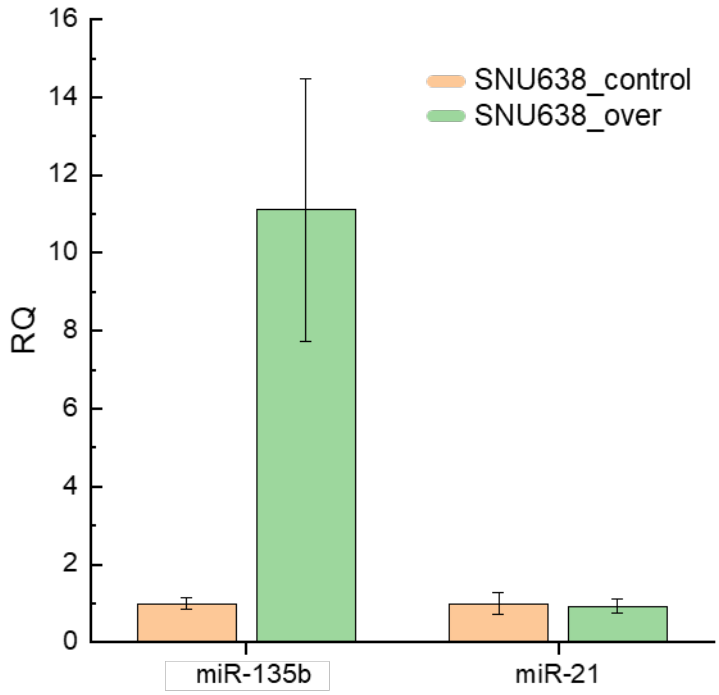

Figure S10. Real-time PCR analyses of (a) miR-135b and (b) miR-21 expression levels in mouse tumor tissues. Expression levels of the miRNAs were normalized to that of RNU6B (n = 3). RQ, Relative quantification.

Table S1. Oligonucleotide sequences used in this study.

Sequence Name	Oligonucleotide sequences (5′–3′)
135b-DNA 1	AAA AAA TCT CAC TAA CT[FAM-dT] ACG G
135b-DNA 2	CCC [BHQ1-dT]AT ATG GCT TTT CAT TCA AAA AA[Acrylamide]
135b-Linker	TCA CAT AGG AAT GAA AAG CCA TAT AGG GCC GTA AGT TAG TGA GA
135b-Fuel	TAA CTT ACG GCC CTA TAT GGC TTT TCA TTC
135b-Target	TAT GGC TTT TCA TTC CTA TGT GA
21-DNA 1	AAA AAA TCT CAC TAA CT[Cy3-dT] ACG G
21-DNA 2	CCC [BHQ2-dT]AT AGC TTA TCA GAC TAA AAA A[Acrylamide]
21-Linker	TCA ACA TCA GTC TGA TAA GCT ATA GGG CCG TAA GTT AGT GAG A
21-Fuel	TAA CTT ACG GCC CTA TAG CTT ATC AGA CT
21-Target	TAG CTT ATC AGA CTG ATG TTG A

Table S2. Summarizing of analytical performances of Janus hydrogel-based FSP.

Samples		FAM (miR-135b) (λ_{ex}: 484 nm , λ_{em}: 530 nm)		CY3 (miR-21) (λ_{ex}: 540 nm , λ_{em}: 579 nm)	
		Mean value (int)	Std. Dev.	Mean value (int)	Std. Dev.
in vitro (n =3)	NIH3T3	9530.5	430.4	9629.0	196.4
	SNU601	20660.2	2307.2	9668.3	643.4
	SNU638	9651.7	871.2	20191.8	1494.9
in vivo (n = 5)	Normal	16503.3	1716.7	17768.9	2857.5
	SNU638_ctrl	15317.2	1710.2	27926.8	3505.3
	SNU638_over	26072.6	3399.1	20933.0	2187.2
clinical sample (n = 15)	Normal	8917.0	1785.8	19419.5	3494.1
	Stage I-II	13781.9	2403.4	21424.0	4574.3
	Stage III-IV	14153.4	3105.7	22419.1	3218.8